Application of Bayesian Designed Artificial Neural Networks in Phase II Structural Health Mentoring Benchmark Studies

Dr. Ching-Tai Ng
School of Civil, Environmental & Mining Engineering,
The University of Adelaide, SA, 5005, Australia,

Abstract

This paper presents the results of a study into the use of pattern recognition as a method for detecting damage in structures. Pattern recognition is achieved by the use of *artificial neural networks* (ANNs); however, these require careful design because the number of hidden layers and the number of neurons in each hidden layer are critical to the ANN's performance. In the current study, a Bayesian model class selection method was employed to select an optimal ANN model class that avoids ad hoc assumptions and subjective decisions in the ANN design. The objective of the research was to provide an extended study of the proposed method using the IASC-ASCE Structural Health Monitoring (SHM) Phase II Simulated Benchmark Structure. Damage-induced modal parameter changes were used as a pattern feature in damage detection. Analysis showed that the proposed method is able to successfully identify damages in a benchmark structure.

Keywords: Structural health monitoring; artificial neural network; Bayesian model class selection method; damage detection; pattern recognition; SHM benchmark structure

1. Introduction

The safety of structures is an important issue worldwide. It has motivated much research, especially into the development of damage detection techniques, each of which offers advantages and disadvantages (Brownjohn 2007; Ng *et al*. 2009; Nichols *et al*. 2011; Ng 2011; Ng & Veidt 2011; Shih *et al*. 2011; Veidt & Ng 2011; Kaphle *et al*. 2012). Some techniques, for example, are sensitive to small damages, but are unsuitable for the global monitoring of structures (Ng *et al*. 2009; Moll & Fritzen 2012; Ng *et al*. 2012; Ng & Veidt 2012).

In the last decade the use of vibration data as an indicator of damage has received significant attention (Hera & Hou 2004; Sohn *et al*. 2004; Yuen *et al*. 2004; Lam *et al*. 2007; Farrar *et al*. 2007). Among the techniques, artificial neural networks (ANNs) have been commonly used in pattern recognition approaches for damage detection. Ni *et al*. (2002) used

an ANN for damage detection following a two-stage approach. Damage locations were identified in stage one and the severity of the damage was determined in stage two. A damage signature index, calculated using natural frequencies and modeshapes, was used as a pattern feature for damage detection. Yuen and Lam (2006) proposed an ANN-based damage detection method in which the ANN was designed using a Bayesian approach. A damage signature vector, calculated using the damage-induced change of natural frequencies and modeshapes, was used as the pattern feature. Bakhary *et al*. (2007) proposed a damage detection method using a statistical ANN with consideration of uncertainties. Natural frequencies and modeshapes were used as the pattern feature. The accuracy of the method was evaluated using Monte Carlo simulation.

Lam and Ng (2008) proposed an extended Bayesian design algorithm to provide a mathematically rigorous approach for designing an ANN for structural damage detection. Two pattern features were compared using the IASC-ASCE Structural Health Monitoring (SHM) Phase I Simulated Benchmark Structure. The pattern features were damage-induced change of natural frequencies and modeshapes, and damage-induced change of Ritz vectors. They showed that the performance of the ANN trained by the damage-induced change of natural frequencies and modeshapes was slightly better than that of the ANN trained by the damage-induced change of Ritz vectors.

The damages considered in the Phase I SHM benchmark problem are relatively large, which makes the problem less realistic. The main objective of the current study was to extend the study of Lam and Ng (2008) to the Phase II SHM benchmark problem, which considers smaller damages and less contrived situations in damage detection. The study provides a comprehensive and practical verification for the proposed methodology.

The remainder of this paper is organised as follows. The extended Bayesian ANN design algorithm is presented in Section 2. A description of the Phase II benchmark structure is provided in Section 3. The damage detection results using the Bayesian designed ANN are then reported and discussed in detail. Finally, conclusions are drawn in Section 4.

2. Proposed Methodology

2.1. Pattern recognition approach

Pattern recognition is a promising approach for damage detection. The fundamental idea of the approach is to use a set of prescribed quantities, such as natural frequencies and modeshapes, as pattern features for each possible damage pattern of a structure. In damage detection the pattern features for all possible damage patterns of the structure can be generated by computer simulations and then used to construct a comprehensive database. Once the measured pattern feature of the damaged structure is obtained from dynamic measurements, the feature is compared to all the calculated pattern features in the database.

The damage pattern corresponding to the best match is treated as the most probable damage pattern.

One of the advantages of the pattern recognition approach is that the damage detection process does not require any modal expansion and/or matrix condensation. However, the pattern recognition approach requires a very large database to store all possible damage patterns, especially for large scale structures; and the matching of the measured pattern feature to all calculated pattern features is computationally very intensive. In this paper an ANN is proposed to address the aforementioned difficulties of the pattern recognition approach.

2.2.Pattern feature

In the current study the damage-induced changes of modal parameters are employed as the pattern features, which are used as the inputs in the ANN training process. A set of input-target training data can be generated by computer simulations. The damage-induced changes of modal parameters for different damage cases can be calculated by

$$\begin{aligned} \mathrm{PF}(k) = &\left[\boldsymbol{\Phi}_1^T(k),...,\boldsymbol{\Phi}_{N_F}^T(k),\omega_1(k),...,\omega_{N_F}(k)\right]^T \\ &-\left[\boldsymbol{\Phi}_1^T(0),...,\boldsymbol{\Phi}_{N_F}^T(0),\omega_1(0),...,\omega_{N_F}(0)\right]^T \end{aligned} \tag{1}$$

where $\omega_q(k)$ and $\boldsymbol{\Phi}_q(k)$ are the q-th natural frequency and modeshape, respectively, and $q=1,...,N_F$. N_F is the number of the vibration modes considered in damage detection; $k=1,...,N$ is the index that represents a particular damage case and $k=0$ stands for the undamaged reference case. Each $\mathrm{PF}(k)$ corresponds to a damage index vector

$$\mathrm{DI}(k) = \left[E_1, E_2, ..., E_r, ..., E_{N_D}\right]^T \tag{2}$$

where E_r is the damage severity at the r-th possible damage location. The value of E_r varies from 0 to 100, representing the percentage reduction in stiffness at each damage location. N_D is the total number of possible damage locations. Using the $\mathrm{PF}(k)$ and $\mathrm{DI}(k)$ as the input-target pairs for the ANN training, the trained ANN can then be used to predict the stiffness reduction at each damage location.

2.3.Damage detection using artificial neural network

A multi-hidden-layer feedforward ANN is adopted as a systematic tool for matching the measured pattern features to the calculated pattern features in this study. Before the ANN can be applied to identify the most possible damage pattern, it needs to be trained by a set of calculated pattern features associated with a variety of damage patterns. One of the advantages of an ANN is that it can approximate the most possible damage pattern even though the true damage pattern is not encountered during ANN training. Hence, not all

possible damage patterns need to be considered during ANN training. Figure 1 shows the structure of a multi-hidden-layer feedforward ANN that consists of a number of interconnected simple processing units named artificial neurons, a layer of input unit, N_H layers of hidden units and one layer of output units.

The performance of the damage detection using an ANN mainly depends on the design of the ANN, which involves the selection of the number of hidden layers and hidden neurons in each hidden layer, and the transfer function for all of the neurons in the hidden layers. The number of neurons in the hidden layer and the transfer function has a significant effect on the performance of the ANN and the capability of the ANN to generalise as proved by Yuen and Lam (2006) and Lam and Ng (2008).

In this study a linear function is always employed as the transfer function in the output layer. Cybenko (1989) has proved that only a single hidden layer of an ANN is able to approximate any functional relationship between inputs and outputs. Without loss of generality, the ANN adopted in this study has only a single hidden layer. Designing the ANN, therefore, involves choosing (1) the optimal number of neurons in the hidden layer and (2) the optimal transfer function for all of the neurons in the hidden layer. The selection of the optimal number of neurons in the hidden layer is a challenging issue if selection criteria are based on the discrepancy between the ANN outputs and the targets. The greater the number of neurons in the hidden layer, the less the discrepancy.

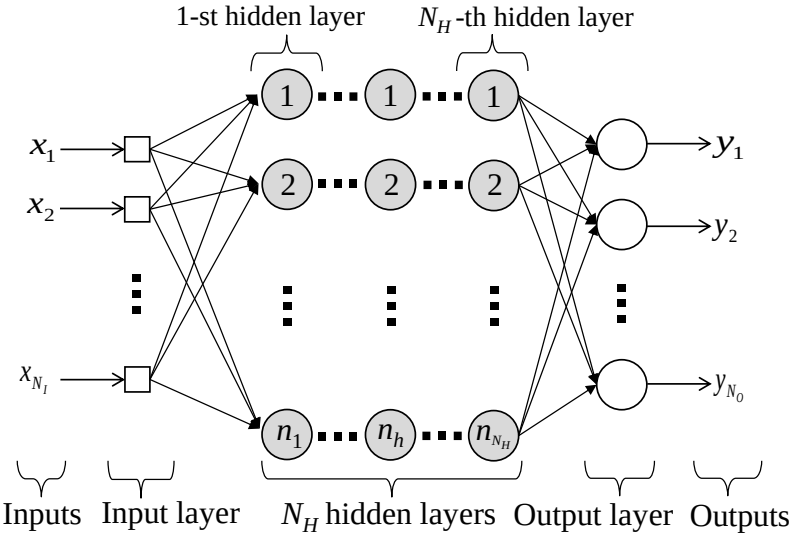

Figure 1: Structure of the multi-hidden-layer feedforward ANN

2.4. Extended Bayesian ANN design algorithm

An extended Bayesian ANN design algorithm (Lam & Ng 2008) is employed to choose the optimal transfer function and the optimal number of neurons in the hidden layer in the current study. The ANN design algorithm is based on the Bayesian model class selection method,

which is briefly reviewed here. Interested readers are referred to Lam and Ng (2008) for more detail.

Bayesian model class selection basically uses a set of input-target training pairs D to select the 'best' ANN model class from M_j model classes, for $j = 1, 2, ..., N_M$. In this study different classes of ANN models correspond to ANNs with different transfer functions and different quantities of neurons in the hidden layer. A vector of the ANN parameters, which includes the weights and biases of the ANN, for a class of ANN model M_j is defined as $\boldsymbol{\theta}_j \in \Re^{N_j}$. For each ANN model class M_j, the training process is to select an ANN model $\boldsymbol{\theta}_j$ such that the ANN can simulate the input-target relation specified by the training data set D. The dimension of the $\boldsymbol{\theta}_j$ is N_j, that is, equal to the number of ANN parameters in each model class M_j. The updated probability density function (PDF) $p(\boldsymbol{\theta}_j \mid D, M_j)$ based on the set of input-target training data can be obtained using Bayes' theorem as (Beck & Katafygiotis 1998)

$$p\left(\boldsymbol{\theta}_j \mid D, M_j\right) = c_j\, p\left(D \mid \boldsymbol{\theta}_j, M_j\right) p\left(\boldsymbol{\theta}_j \mid M_j\right) \tag{3}$$

where $p(\boldsymbol{\theta}_j \mid M_j)$ is the prior (initial) PDF of $\boldsymbol{\theta}_j$ that allows engineering judgment of the plausibility of the different sets of $\boldsymbol{\theta}_j$ to be incorporated. c_j is a normalising constant and $p(D \mid \boldsymbol{\theta}_j, M_j)$ is the likelihood, which is assumed to be independent of Gaussian prediction errors. The likelihood can be expressed as

$$p\left(D \mid \boldsymbol{\theta}_j, M_j\right) = \left(\sqrt{2\pi}\sigma_\eta\right)^{-NN_O} \exp\left[-\frac{NN_O}{2\sigma_\eta^2} J\left(\boldsymbol{\theta}_j \mid D, M_j\right)\right] \tag{4}$$

where N is the total number of input-target training pairs and N_O is the number of output neurons of the ANN. σ_η is the optimal standard deviation of the target error. The contribution of the training data to the likelihood is $J(\boldsymbol{\theta}_j \mid D, M_j)$, which is defined as

$$J\left(\boldsymbol{\theta}_j \mid D, M_j\right) = \frac{1}{NN_O} \sum_{k=1}^{N} \left\| y\left(k; \boldsymbol{\theta}_j, M_j\right) - \hat{y}\left(k\right) \right\|^2 \tag{5}$$

where $y(k; \boldsymbol{\theta}_j, M_j)$ is the ANN output corresponding to the *k*-th input for a given set $\boldsymbol{\theta}_j$ of the model class M_j. $\hat{y}(k)$ is the target of the ANN for the *k*-th input. $\|\cdot\|$ is the Euclidean norm of a vector. The value of $J(\boldsymbol{\theta}_j \mid D, M_j)$ shows the performance of the ANN. The optimal ANN parameter vector $\hat{\boldsymbol{\theta}}_j$ can be obtained by minimising $J(\boldsymbol{\theta}_j \mid D, M_j)$.

The 'best' ANN model class can be determined by calculating the probability of the model class M_j conditional on the set of input-target training data D which can be obtained using the Baye's theorem again (Beck & Yuen 2004; Lam *et al*. 2009).

$$p\left(M_j \mid D, U\right) = \frac{p\left(D \mid M_j, U\right) p\left(M_j \mid U\right)}{p\left(D \mid U\right)} \quad \text{for } j = 1, ..., N_M \tag{6}$$

where $p(D|U)=\sum_{j=1}^{N_M} p(D|M_j,U)P(M_j|U)$ by the theorem of total probability and U expresses the user's judgment on the initial plausibility of the ANN model classes, expressed as a prior probability $P(M_j|U)$ of the ANN model classes M_j for $j=1,\ldots,N_M$, where $\sum_{j=1}^{N_M} P(M_j|U)=1$. The factor $p(D|M_j,U)$ is called the evidence of the ANN model class M_j provided by the data D.

One of the objectives is to calculate the value of the probability in Equation (6) for a given ANN model class M_j. As a result, the relative plausibility among different classes of ANN models (e.g., M_1, M_2, …, M_{N_M}), in which each M_j is the ANN model with a different transfer function and number of neurons in the hidden layer, can be quantified. The optimal ANN model class is the one having the maximum value of $p(D|M_j,U)$. The evidence of the ANN model class M_j can be calculated using an asymptotic approximation (Papadimitriou *et al*. 1997) as

$$p(D|M_j)\approx(2\pi)^{\frac{N_j}{2}}\, p(\hat{\boldsymbol{\theta}}_j|M_j)\,p(D|\hat{\boldsymbol{\theta}}_j,M_j)\left|\mathbf{H}_j(\hat{\boldsymbol{\theta}}_j)\right|^{-\frac{1}{2}} \quad \text{for } j=1,\ldots,N_M \qquad (7)$$

where $\hat{\boldsymbol{\theta}}_j$ is the optimal ANN parameter vector that can be obtained by maximising the posterior PDF $p(\boldsymbol{\theta}_j|D,M_j)$ in Equation (3) and $\mathbf{H}_j(\hat{\boldsymbol{\theta}}_j)$ is the Hessian matrix of the function $g(\boldsymbol{\theta}_j)=-\ln[p(\boldsymbol{\theta}_j|M_j)p(D|\boldsymbol{\theta}_j,M_j)]$.

3. Phase II IASC-ASCE SHM Benchmark Structure

The Phase II IASC-ASCE SHM benchmark structure is briefly summarised here. The benchmark structure considers a three-dimensional (3D) finite element (FE) structural model written using the MATLAB program (Bernal *et al*. 2002). The model is a four-storey, 2×2 bay steel frame with 120 degrees-of-freedom (DOF). The base of the structure is fixed. The *x*-direction is the strong direction of the columns.

The nominal masses are 3242kg, 2652kg, 2652kg and 1809kg for the 1st to the 4th storey, respectively. It is assumed that all floors are rigid in the *x*-*y* plane. The Phase II simulated benchmark problem considers the modelling uncertainties by randomly selecting all floor masses and brace stiffnesses with ±10% and ±5% uncertainty, respectively, with a uniform distribution assumption. The centre of the floor mass in the benchmark problem deviates from the geometrical floor centre. The deviation is simulated by randomly selecting a factor from a uniform distribution over [-0.05 0.05] of the floor width.

Six simulated damages of different severity and at different locations are considered in this study. They are summarised below.

(i) Case DP1B: 50% stiffness reduction in two braces at the 1st storey (dashed lines in Figure 2a)

(ii) Case DP2B: same as in Case DP1B, but with a stiffness reduction of 25%

(iii) Case DP3B: same damaged braces as in Case DP1B at the 1st storey, but having two additional braces with 25% stiffness reduction at the 3rd storey (dashed lines in Figure 2b)

(iv) Case DP3Ba1: 50% and 25% stiffness reduction in a brace at the 1st and 3rd storey (dashed lines in Figure 2c), respectively; an asymmetric damage situation

(v) Case DP3Ba2: same damaged braces as in Case DP3Ba1, but 35% and 15% stiffness reduction in a brace at the 1st and 3rd storeys (dashed lines in Figure 2c), respectively.

(vi) Case DP3Ba3: same damaged braces as in Case DP3Ba1, but a 20% and 10% stiffness reduction in a brace at the 1st and 3rd storeys (dashed lines in Figure 2c), respectively.

It should be noted that Cases DP3Ba1, DP3Ba2 and DP3Ba3 do not belong to the Phase II IASC-ASCE SHM benchmark problem (Bernal *et al*. 2002). They are additional cases designed to provide a more challenging situation in the proposed methodology verification.

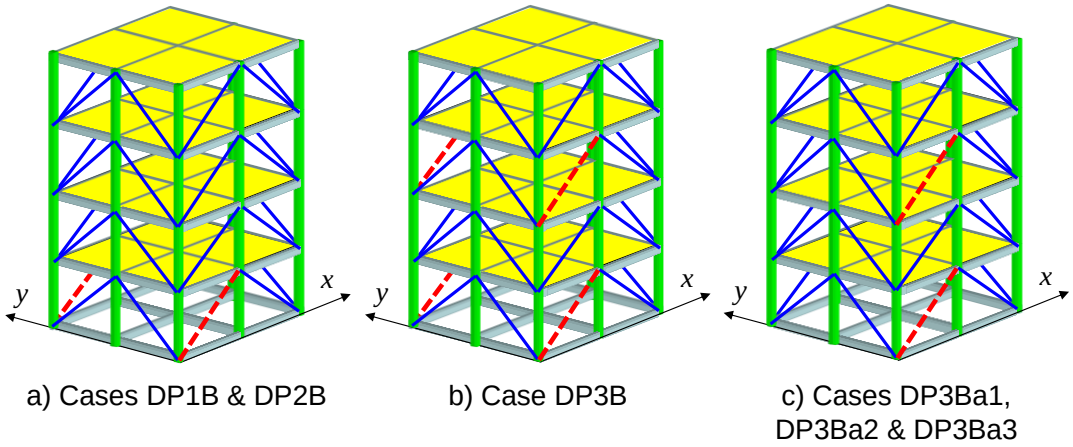

a) Cases DP1B & DP2B b) Case DP3B c) Cases DP3Ba1, DP3Ba2 & DP3Ba3

Figure 2: Damage pattern for all cases (dashed lines indicate the damaged braces)

Table 1: Actual percentage reduction in horizontal stiffness of each storey for each damage case

Case	Dir.	Storey			
		1st	2nd	3rd	4th
DP1B	*x*	**11.31**	0.00	0.00	0.00
	y	0.00	0.00	0.00	0.00
DP2B	*x*	**5.66**	0.00	0.00	0.00
	y	0.00	0.00	0.00	0.00
DP3B	*x*	**11.31**	0.00	**5.66**	0.00
	y	0.00	0.00	0.00	0.00
DP3Ba1	*x*	**5.66**	0.00	**2.83**	0.00
	y	0.00	0.00	0.00	0.00
DP3Ba2	*x*	**3.96**	0.00	**1.70**	0.00
	y	0.00	0.00	0.00	0.00
DP3Ba3	*x*	**2.26**	0.00	**1.13**	0.00
	y	0.00	0.00	0.00	0.00

Table 1 shows the actual percentage reductions in the horizontal stiffness of each storey for each case of damage in the *x*- and *y*-direction. The percentages are calculated based on the aforementioned stiffness reduction in each case of damage. The maximum and minimum percentage of horizontal stiffness reductions are 11.31% and 1.13%, respectively. Table 2 shows the nominal natural frequencies and damping ratios for the undamaged reference case (RB) and the damage cases, which are calculated using the nominal mass and stiffness of the benchmark structure. 1% modal damping is assumed for each mode. Because the *x*-direction is the strong direction for the columns of the benchmark structure, the first (1x) and second (2x) modes of natural frequency in the *x*-direction have higher frequencies than the first and second modes in the *y*-direction.

Table 2: Nominal modal parameters

Case	Natural frequency (Hz)				Damping ratio (%)			
	1x	2x	1y	2y	1x	2x	1y	2y
RB	8.74	25.29	8.35	23.15	1.00	1.00	1.00	1.00
DP1B	8.44	24.55	8.35	23.15	1.00	1.00	1.00	1.00
DP2B	8.60	24.93	8.35	23.15	1.00	1.00	1.00	1.00
DP3B	8.36	24.72	8.35	23.15	1.00	1.00	1.00	1.00
DP3Ba1	8.55	24.72	8.35	23.15	1.00	1.00	1.00	1.00
DP3Ba2	8.61	24.92	8.35	23.15	1.00	1.00	1.00	1.00
DP3Ba3	8.67	25.07	8.35	23.15	1.00	1.00	1.00	1.00

A broadband stationary excitation is applied to each floor of the structure to generate the ambient vibration data. It is assumed that there is an accelerometer installed in the centre of each side of each floor with the measurement direction parallel to the side in either the positive *x*- or *y*-direction. The dynamic problem is solved by a time history integration method using MATLAB's *lsim* command, which uses a discrete time integration algorithm that assumes excitation is constant over a time step. The time histories of the sampling interval are 0.001s, and the total duration is 210s for the undamaged reference case and all damage cases. The first 10s is ignored as it contains transient responses due to the stationary excitation at the beginning, during the generation of the simulated data. The damping ratio is assumed to be 1% for all vibration modes. The level of the measurement noise is 10% RMS of the actual acceleration responses and the noise is generated using independent Gaussian pulse processes. The simulated acceleration responses are then used in the modal identification, discussed in Section 3.2.

3.1. ANN design

A 3D 12-DOF shear building model is employed to generate the input-target ANN training data for damage-induced horizontal stiffness reduction in the *x*- and *y*- direction. There are four possible damage locations in either the *x*- or *y*-direction, and the damages are

represented as a reduction in inter-storey stiffness. Because the measured acceleration responses are simulated using the 3D 120-DOF FE model, the effect of modelling error is considered in addition to the modelling uncertainties in the benchmark structure. It is assumed that the brace damages can occur on every storey and reduce the horizontal inter-storey stiffness in either the *x*- or *y*-direction. There are, therefore, four possible damage locations in each direction.

At each storey only five damage levels of stiffness reduction, 0%, 20%, 40%, 60% and 80%, are considered, along with only two out of four simultaneous damages in each direction in generating the input-target ANN training data. The total number of damage patterns to be examined in each direction is 113. The set of input-target training data can then be used to design and train two ANNs as proposed in Section 2.4. The ANNs for detecting damages in the *x*- and *y*-direction are named ANNx and ANNy, respectively. ANNs with different quantities of neurons in the hidden layer are considered in the ANN design process. Using the extended Bayesian ANN design algorithm noted in Section 2.4, the ANNx and ANNy with the tangent sigmoid transfer function and 17 neurons in the hidden layer have the maximum logarithm of evidence (1588.67 for ANNx and 1575.67 for ANNy). They are therefore selected to detect damages in the benchmark problem. Interested readers are referred to Lam and Ng (2008) for the details of the ANN design.

3.2. Identified modal parameters

The first four translation modes (two in the *x*-direction and two in the *y*-direction) are identified from ambient vibration responses using MODE-ID (Beck *et al*. 1994), which is a nonlinear least-squares method based on a linear dynamical model with classical normal modes of vibration. The identified natural frequencies and damping ratios are shown in Table 3. The frequencies are close to the nominal values as recorded in Table 2. The identified mass normalised modeshapes of the undamaged reference case and the cases of damage in the *x*- and *y*- direction are shown in Figures 3 and 4, and Figures 5 and 6, respectively. The modal assurance criteria (MAC) (Allemang & Brown 1982) are employed to ensure the correct modes are matched as the order of the vibration modes may change after the structure is damaged. Table 3 and Figures 3 to 4 show that there is a small change in the identified modal parameters for the damaged structure in all cases of damage compared to the nominal modal parameters in Table 2. The identified natural frequencies and mass-normalised modeshapes are used to calculate the damage-induced changes of modal parameters, and are then input to the trained ANNx and ANNy to identify the horizontal stiffness reductions in the *x*- and *y*-direction for each case of damage.

Table 3: Identified modal parameters

Case	Natural frequency (Hz)				Damping ratio (%)			
	1x	2x	1y	2y	1x	2x	1y	2y
RB	8.74	25.33	8.34	23.17	1.04	1.09	0.89	1.17
DP1B	8.46	24.54	8.34	23.16	1.26	1.20	0.89	1.17
DP2B	8.59	24.92	8.34	23.17	0.88	0.99	0.89	1.17
DP3B	8.34	24.20	8.34	23.17	0.96	0.91	0.88	1.17
DP3Ba1	8.54	24.71	8.34	23.16	0.79	0.84	0.91	1.19
DP3Ba2	8.61	24.92	8.34	23.16	0.97	1.12	0.91	1.19
DP3Ba3	8.65	25.08	8.33	23.16	1.13	1.03	0.91	1.19

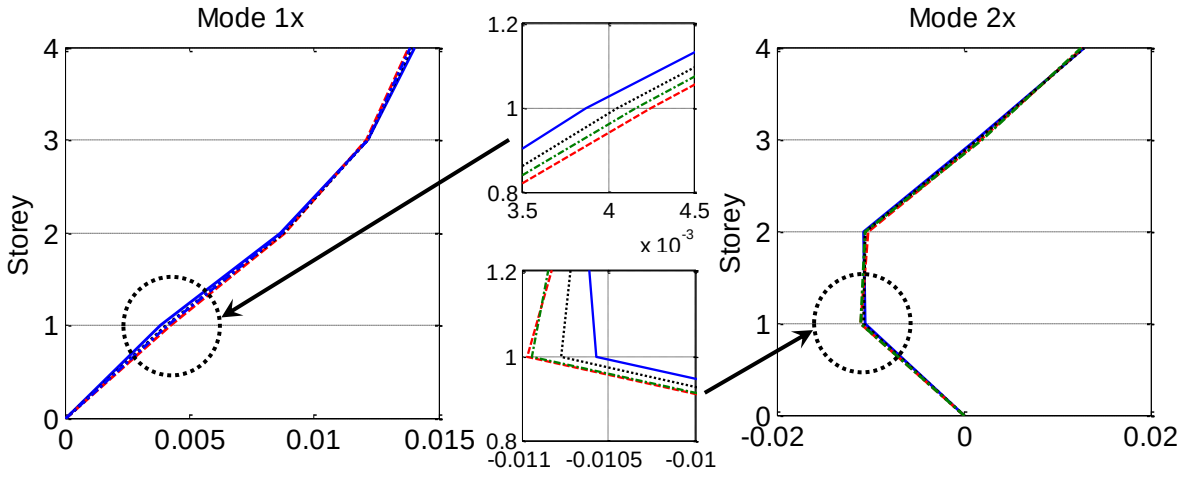

Figure 3: Identified mass-normalised modeshapes in the *x*-direction and zoom-in at the 1st storey for Cases RB, DP1B, DP2B and DP3B (solid lines: Case RB; dashed lines: Case DP1B; dotted lines: Case DP2B; dash-dotted lines: Case DP3B)

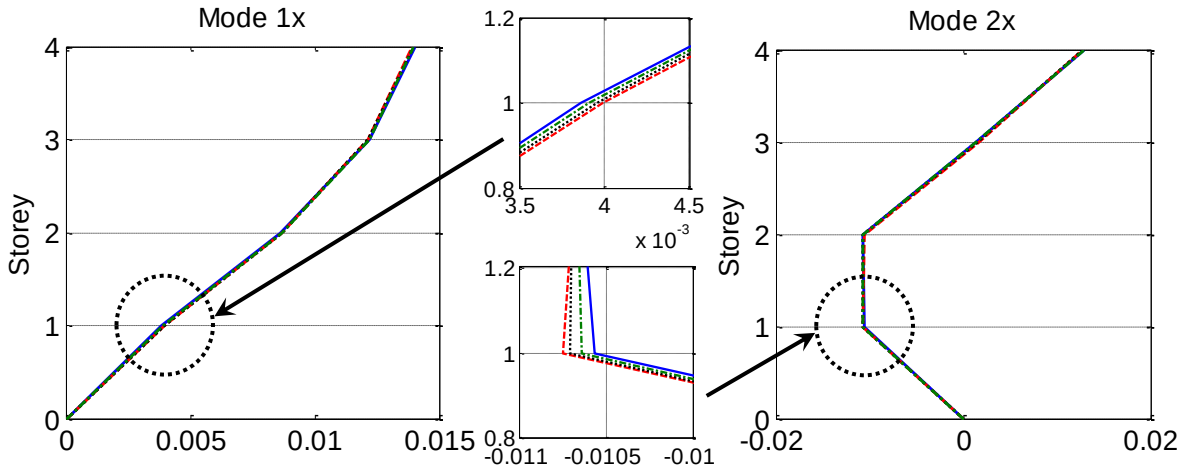

Figure 4: Identified mass-normalised modeshapes in the *x*-direction and zoom-in at the 1st storey for Cases RB, DP3Ba1, DP3Ba2 and DP3Ba3 (solid lines: Case RB; dashed lines: Case DP3Ba1; dotted lines: Case DP3Ba2; dashed-dotted lines: Case DP3Ba3)

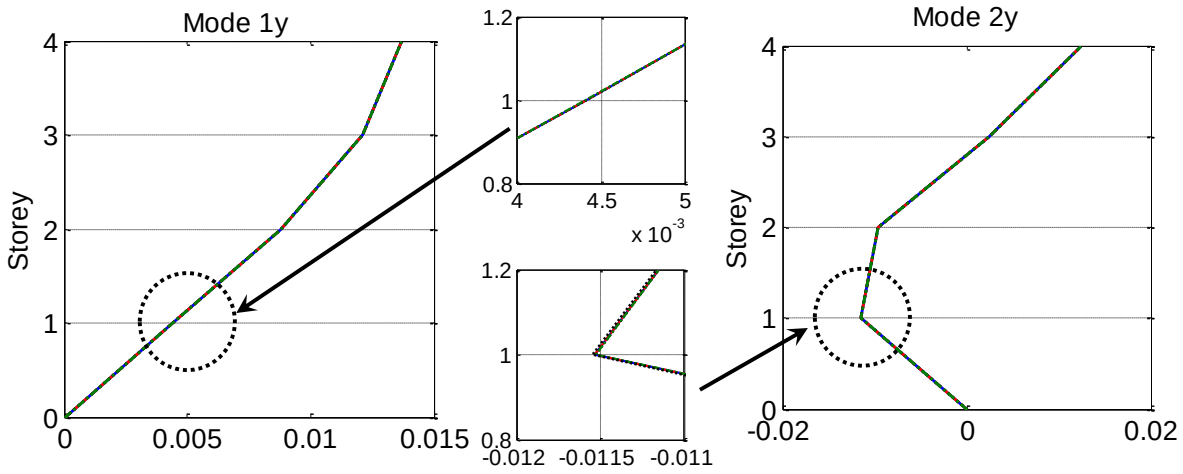

Figure 5: Identified mass-normalised modeshapes in the *y*-direction and zoom-in at the 1st storey for Cases RB, DP1B, DP2B and DP3B (solid lines: Case RB; dashed lines: Case DP1B; dotted lines: Case DP2B; dash-dotted lines: Case DP3B)

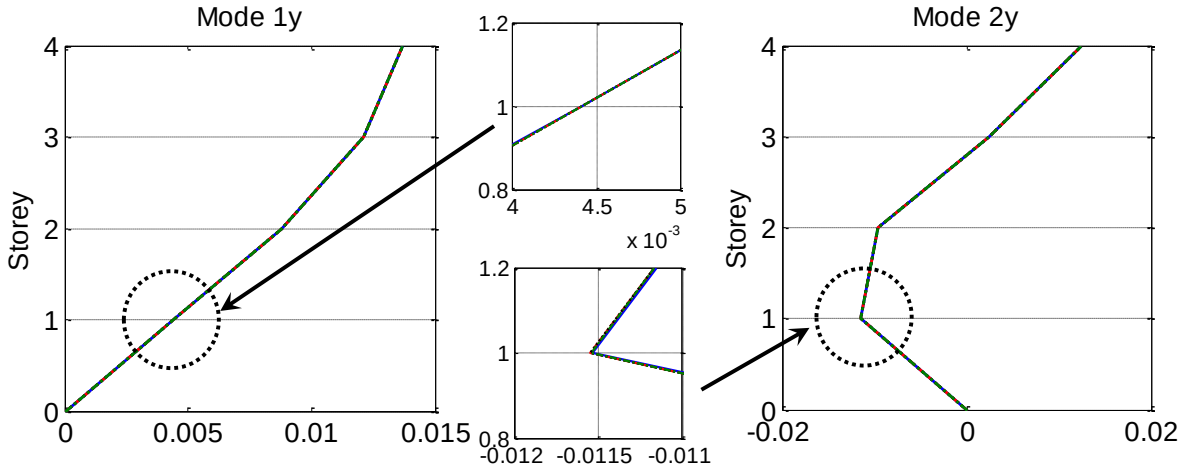

Figure 6: Identified mass-normalised modeshapes in the *y*-direction and zoom-in at the 1st storey for Cases RB, DP3Ba1, DP3Ba2 and DP3Ba3 (solid lines: Case RB; dashed lines: Case DP3Ba1; dotted lines: Case DP3Ba2; dashed-dotted lines: Case DP3Ba3)

3.3.Damage identification results

The trained ANNx and ANNy are used to identify the stiffness reductions in the *x*- and *y*-directions, respectively. Table 4 shows the identified percentage stiffness reductions for all damage cases. Case DP1B considers an 11.31% horizontal stiffness reduction at the first storey. The damage detection results show that the horizontal stiffness reduction at the 1st storey in the *x*-direction is 10.96%, which is very close to the actual value shown in Table 1. For those storeys without any damage, the identified percentage reductions in horizontal

stiffness are either zero or a very small number, such as 0.2% at the 2nd storey in the *x*-direction and 0.07 at the 3rd storey in the *y*-direction. Case DP2B considers a smaller stiffness reduction at the 1st storey. The identified stiffness reduction is 5.79%. It is very close to the actual value 5.66%.

Cases DP3B, DP3Ba1, DP3Ba2 and DP3Ba3 consider more challenging situations. There are a 11.31% and 5.66% stiffness reduction at the 1st and 3rd storey in the *x*-direction in Case DP3B. Cases DP3Ba1, DP3Ba2 and DP3Ba3 consider smaller stiffness reductions at the same damaged storeys as Case DP3B. However, there is only a brace damaged at the 1st and 3rd storeys in this case, making it a case of asymmetric damage. Case DP3Ba3 is the most challenging case. There is only 2.26% and 1.13% stiffness reduction in the 1st and 3rd storeys.

The results in Table 4 show that the identified stiffness reductions are close to the actual values of Cases DP3B, DP3Ba1, DP3Ba2 and DP3Ba3 as shown in Table 1. If 1% stiffness reduction is considered to be the threshold value for damage, then only one false indicator out of 48 indicators – the 1.20% stiffness reduction in the 2nd storey of Case DP3B – appears in the identified results as shown in Table 4. In addition, the proposed method does not "miss" any damage, and the damage detection results are on the safe side. It can be concluded therefore that the proposed method performs well in terms of damage detection in a Phase II SHM simulated benchmark structure.

Table 4: Identified percentage reduction in horizontal stiffness

Case	Dir.	Storey			
		1st	2nd	3rd	4th
DP1B	*x*	**10.96**	0.20	0.00	0.00
	y	0.00	0.00	0.07	0.00
DP2B	*x*	**5.79**	0.54	0.00	0.00
	y	0.00	0.00	0.00	0.03
DP3B	*x*	**11.38**	1.20	**6.22**	0.00
	y	0.00	0.00	0.01	0.06
DP3Ba1	*x*	**6.23**	0.60	**2.90**	0.00
	y	0.04	0.00	0.12	0.00
DP3Ba2	*x*	**4.12**	0.48	**1.82**	0.00
	y	0.02	0.00	0.09	0.00
DP3Ba3	*x*	**2.54**	0.65	**1.23**	0.00
	y	0.03	0.00	0.10	0.00

4. Conclusions

A pattern recognition approach using an ANN is employed to detect damages in a Phase II IASC-ASCE SHM simulated benchmark structure. The proposed method uses an extended Bayesian ANN design algorithm to select the optimal ANN model class for damage detection. Six cases of damage are considered in this study. The results of the damage detection are very

encouraging. All of the identified stiffness reductions are very close to the actual values.

5. References

Allemang, R.J. and Brown, D.L. (1982). A correlation coefficient for modal vector analysis. In *Proceedings of the 1st IMAC*, 110-116.

Bakhary, N. Hao, H. and Deeks, A.J. (2007). Damage detection using artificial neural network with consideration of uncertainties. *Engineering Structures*, 29: 2806-2815.

Beck, J.L. and Katafygiotis, L.S. (1998). Updating models and their uncertainties I: Bayesian statistical framework. *Journal of Engineering Mechanics, ASCE*, 124: 455-461.

Beck, J.L. and Yuen, K.V. (2004). Model selection using response measurement: A Bayesian probabilistic approach. *Journal of Engineering Mechanics, ASCE*, 130: 192-203.

Beck, J.L., May, B.S. and Polidori, D.C. (1994). Determination of modal parameters form ambient vibration data for structural health monitoring. In *Proceedings of the 1st World Conference on Structural Control*, TA3:3-12.

Bernal, D., Dyke, S.J., Beck, J.L. and Lam, H.F. (2002). Phase II of the ASCE benchmark study on structural health monitoring. In *Proceedings of the 15th Engineering Mechanics Division Conference of the American Society of Civil Engineers*, New York, US.

Brownjohn, J.M.W. (2007). Structural health monitoring of civil infrastructure. *Philosophical Transactions of the Royal Society A: Mathematical Physical & Engineering Sciences*, 365: 589-622.

Ching, J. and Beck, J.L. (2004). New Bayesian model updating algorithm applied to a structural health monitoring benchmark. *Structural Health Monitoring*, 3: 313-332.

Cybenko, G. (1989). Approximation by superpositions of a sigmoidal function. *Mathematics of Control, Signals and Systems*, 2: 303-314.

Farrar, C.R. and Worden, K. (2007). An introduction to structural health monitoring. *Philosophical Transactions of the Royal Society A: Mathematical Physical & Engineering Sciences*, 2007. 365: 303-315.

Hera, A. and Hou Z. (2004). Application of wavelet approach for ASCE structural health monitoring benchmark studies. *Journal of Engineering Mechanics, ASCE*, 130: 96-104.

Kaphle, M., Tan, A.C.C., Thambiratnam, D.P. and Chan, T.H.T. (2012). Identification of acoustic amission wave modes for accurate source location in plate-like structures. *Structural Control and Health Monitoring*, 19: 197-198.

Lam, H.F. and Ng, C.T. (2008). The selection of pattern features for structural damage detection using an extended Bayesian ANN algorithm. *Engineering Structures*, 30: 2762-2770.

Lam, H.F., Ng, C.T. and Leung, A.Y.T. (2007). Multi-crack detection on semi-rigidly connected beams utilizing dynamic data. *Journal of Engineering Mechanics, ASCE*, 134: 90-99.

Lam, H.F., Ng, C.T., Lee, Y.Y. and Sun, H.Y. (2009). System identification of an enclosure with leakages using a probabilistic approach. *Journal of Sound and Vibration*, 322: 756-771.

Moll, J. and Fritzen, C.P. (2012). Guided waves for autonomous online identification of structural defects under ambient temperature variations. *Journal of Sound and Vibration*, 331: 4587-4597.

Ng, C.T. (2011). Probabilistic methods for structural safety evaluation, damage detection and reliability analysis of structures. *VDM Verlag Dr. Muller GmbH & Co. KG*.

Ng, C.T. and Veidt, M. (2011). Scattering of the fundamental anti-symmetric Lamb wave at delamination in composite laminates. *The Journal of Acoustical Society of America*, 129: 1288-1296.

Ng, C.T. and Veidt, M. (2012). Scattering characteristics of Lamb waves from debondings at structural features in composite laminate. *The Journal of Acoustical Society of America*, 132: 115-123.

Ng, C.T., Veidt, M. and Lam, H.F. (2009). Guided wave damage characterisation in beams utilising probabilistic optimisation. *Engineering Structures*, 31: 2842-2850.

Ng, C.T., Veidt, M. and Rajic, N. (2009). Integrated piezoceramic transducers for imaging damage in composite laminates. *Proceedings of SPIE*, 7493(74932M): 1-8.

Ng, C.T., Veidt, M. Rose, L.R.F. and Wang, C.H. (2012). Analytical and finite element prediction of Lamb wave scattering at delamination sin quasi-isotropic composite laminates. *Journal of Sound and Vibration*, 331: 4870-4883.

Ni, Y.Q., Wong, B.S. and Ko, J.M. (2002). Constructing input vectors to neural networks for structural damage identification. *Smart Materials and Structures*, 11: 825-833.

Nichols, J.M., Moore, E.Z. and Murphy, K.D. (2011). Bayesian identification of a cracked plate using a population-based Markov Chain Monte Carlo method. *Computers and Structures*, 89: 1323-1332.

Papadimitriou, C. Beck, J.L., Katafygiotis, L.S. (1997). Asymptotic expansion for reliability and moments of uncertain systems. *Journal of Engineering Mechanics, ASCE*, 123: 1219-1229.

Shih, H.W., Thambiratnam, D.P. and Chan, T.H.T. (2011). Damage detection in truss bridges using vibration based multi-criteria approach. *Structural Engineering and Mechanics*, 39: 187-206.

Sohn, H., Farrar, C.R., Hernez, F.M., Czrnecki, J.J., Shunk, D.D., Stinemates, D.W. *et al*. (2004). A review of structural health monitoring literature: 1669-2001, *report no. LA-13976-MS*. Los Alamos (NM): Los Alamos National Laboratory.

Veidt, M. and Ng, C.T. (2011). Influence of stacking sequence on scattering characteristics of the fundamental anti-symmetric Lamb wave at through holes in composite laminates. *The Journal of the Acoustical Society of America*, 129: 1280-1287.

Yuen, K.V. and Lam, H.F. (2006). On the complexity of artificial neural networks for smart structures monitoring. *Engineering Structures* 28: 977-984.

Yuen, K.V., Au, S.K. and Beck, J.L. (2004). Two-stage structural health monitoring approach for Phase I benchmark studies. *Journal of Engineering Mechanics, ASCE*, 130: 16-33.